Hindawi
Complexity
Volume 2018, Article ID 4230649, 10 pages
https://doi.org/10.1155/2018/4230649

WILEY | Hindawi

Research Article

The Measurement and Elimination of Mode Splitting: From the Perspective of the Partly Ensemble Empirical Mode Decomposition

Bin Liu,[1,2,3] **Peng Zheng**,[1,3] **Qilin Dai**,[1,3] **and Zhongli Zhou**[1,3]

[1]*College of Management Science, Chengdu University of Technology, Chengdu, Sichuan Province 610059, China*
[2]*School of Economics and Management, University of Electronic Science and Technology, Chengdu, Sichuan Province 611731, China*
[3]*Geomathematics Key Laboratory of Sichuan Province, Chengdu, Sichuan Province 610059, China*

Correspondence should be addressed to Bin Liu; liubincim@163.com

Received 3 July 2018; Revised 14 September 2018; Accepted 19 September 2018; Published 19 November 2018

Academic Editor: Dimitri Volchenkov

The problems of mode mixing, mode splitting, and pseudocomponents caused by intermittence or white noise signals during empirical mode decomposition (EMD) are difficult to resolve. The partly ensemble EMD (PEEMD) method is introduced first. The PEEMD method can eliminate mode mixing via the permutation entropy (PE) of the intrinsic mode functions (IMFs). Then, bilateral permutation entropy (BPE) of the IMFs is proposed as a means to detect and eliminate mode splitting by means of the reconstructed signals in the PEEMD. Moreover, known ingredient component signals are comparatively designed to verify that the PEEMD method can effectively detect and progressively address the problem of mode splitting to some degree and generate IMFs with better performance. The microseismic signal is applied to prove, by means of spectral analysis, that this method is effective.

1. Introduction

The Hilbert–Huang transform (HHT) method, which is composed of the empirical mode decomposition (EMD) and the Hilbert transform (HT) [1, 2], has been proved to be an innovative and a valid approach to dealing with nonlinear and nonstationary data [3]. As an adaptive time-frequency data analysis method, the EMD has been widely applied to numerous fields [4–6]. Multiple improved theories based on the EMD have been proposed as solutions to the problems in EMD algorithms, including mode mixing and pseudo-IMFs. For example, the ensemble EMD (EEMD) has been proposed as a means to essentially resolve the mode-mixing problem associated with EMD and added noises [7]. Additionally, the complementary EEMD (CEEMD) [8] has been proposed as a means to improve the efficiency of the original noise-assisted method by adding noises in pairs with plus and minus signs, which aims to reduce the reconstruction errors caused by the added white noises. The improved theories mentioned above seek to eliminate mode mixing and pseudo-IMFs by changing the initial condition in the EMD algorithm before the partly ensemble EMD (PEEMD) method is applied. By introducing the permutation entropy (PE) of the IMFs, the researchers may judge, via the PEEMD method, whether there are noise signals in the IMFs [9] and then exclude the noise signals from the targeted signals with the expectation that no mode mixing exists in the construction of the targeted signals.

The permutation entropy (PE) [10] is proposed as a means to measure the complexity of the time series. The complexity of the time series can be examined via several other approaches, such as the approximate entropy [11], sample entropy [12], Shannon entropy [13], or cross-sample entropy [14]. Unlike the approximate entropy, sample entropy, and Shannon entropy, the PE estimates the complexity of the time series by comparing the neighboring values. The PE has been widely used in many areas, such as electroencephalography (EEG) signal analysis [15], predicting behavioral actions [16], stock market analysis and

financial dynamics [17, 18], and breakage detection in mechanical systems [19]. Later, the multiscale permutation entropy was introduced into price models [20] and to the medical field [21].

After being used as a robust tool to measure the complexity of the arbitrary time series, the PE was also utilized to estimate the randomness or stationarity of the single IMF in the process of PEEMD. The method of eliminating mode mixing has been transformed into a quantitative assessment approach based on the result of decomposition. To conduct a quantitative research, this paper utilizes the PE to estimate the first and second levels of the IMFs to calculate the bilateral permutation entropy (BPE), thereby progressively eliminating mode splitting. The rest of this paper is organized as follows. Section 2 provides a brief overview of the PEEMD algorithm and the PE algorithm to analyze the mechanisms of mode splitting in IMFs. In Section 3, the proposed method is compared with PEEMD by analyzing synthetic and microseismic signals. Finally, the discussion and conclusion are presented in Section 4.

2. Overviews of the PEEMD and PE

In the PEEMD's improvement of the EMD algorithm, PE is utilized to estimate the randomicity and dynamic changes of the single IMF in the PEEMD algorithm. The PEEMD algorithm and the PE algorithm are presented as follows to introduce the proposed method for accessing mode splitting by the PE value of two or more IMFs.

2.1. PEEMD and Mode Splitting. The PEEMD has greatly solved the problem of mode mixing and overcome the disadvantages of the EEMD and CEEMD. The PEEMD is described as follows [9].

(i) Let $j = 1$, and add the white noise series $\{n_i(t)\}$ and $\{-n_i(t)\}$ to the targeted signal $S(t)$; $S(t)$ is a given time series signal, then

$$\begin{aligned} r_{ij}^{+}(t) &= S(t) - \mathrm{an}_i(t), \\ r_{ij}^{-}(t) &= S(t) - \mathrm{an}_i(t), \end{aligned} \tag{1}$$

where a is the amplitude of added white noise, $i = 1, 2, \ldots, \mathrm{Ne}$ and Ne indicates the pair number of added white noise. j is the number of iterations for decomposing to the IMFs that meet the requirements

(ii) Decompose the two signal series $\{r_{ij}^{+}(t)\}$ and $\{r_{ij}^{-}(t)\}$ using EMD in the jth IMF mode, and two IMF sets $\{I_{ij}^{+}\}$ and $\{I_{ij}^{-}\}$ as well as two residue sets $\{r_{ij+1}^{+}(t)\}$ and $\{r_{ij+1}^{-}(t)\}$ can be obtained, respectively:

$$\begin{aligned} r_{ij+1}^{+}(t) &= r_{ij}^{+}(t) - I_{ij}^{+}(t), \\ r_{ij+1}^{-}(t) &= r_{ij}^{-}(t) - I_{ij}^{-}(t). \end{aligned} \tag{2}$$

(iii) By assembling the final IMF in the jth rank, (3) can be obtained:

$$I_j(t) = \frac{1}{2\mathrm{Ne}} \sum_{i=1}^{\mathrm{Ne}} \left[I_{ij}^{+}(t) + I_{ij}^{-}(t) \right]. \tag{3}$$

(iv) Calculate the PE of $I_j(t)$. If the P_j is larger than θ_0, then $j = j + 1$ and repeat steps (iii)–(v) until P_j is smaller than θ_0. θ_0 is the threshold, which denotes a regular IMF or intermittency or noise signal

(v) Separate the first $j - 1$ IMFs from the original signal, and the residue $r(t)$ is expressed as

$$r(t) = S(t) - \sum_{k=1}^{j-1} I_k(t). \tag{4}$$

(vi) Decompose $r(t)$ completely by using the EMD

$$r(t) = \sum_{k=1}^{n} c_k(t) + r_n(t). \tag{5}$$

(vii) $\{c_k(t)\}$ are seen as the IMFs following the first $j - 1$ IMFs. The initial signal is described as

$$s(t) = \sum_{i=1}^{j-1} I_i(t) + \sum_{k=1}^{n} c_k(t) + r_n(t). \tag{6}$$

A given signal may be decomposed in a way similar to CEEMD in the first $(j - 1)$th IMFs via the PEEMD method; then, instead of assembling and averaging all IMFs, the EMD is used in the remaining ranks. Hence, the PEEMD can reduce the amount of calculation of CEEMD and greatly improve the accuracy of the obtained IMFs. In addition, since one pair of white noises with positive and negative signs is added to the targeted signal, the reconstruction error (RE) may be limited to a negligible level via the PEEMD. That is, the progress of the PEEMD is complete, and the PE is utilized to indicate the chaos degree so that the roots of mode mixing, including intermittency or noise signal, should be eliminated regardless of mode splitting.

2.2. Permutation Entropy. In this PEEMD algorithm, PE is employed to detect the randomicity and dynamic changes of the time series. Reference [10] denotes that it has the advantages of simple definition, fast speed of calculation, and well robustness. According to the permutation entropy (PE) proposed by Bandt and Pompe, the algorithm is illustrated as follows:

(i) Given a time series $\{x_k\}, k = 1, 2, \ldots, N$, the m-dimensional delay embedding vector at time i is defined as

$$x_i^m = \left[x_i, x_{i+\tau}, \ldots, x_{i+(m-1)\tau}\right]. \quad (7)$$

(ii) In (7), m indicates the embedded dimension and τ is the time delay, Then, x_i^m has a permutation $\pi_{r_0 r_1 r_{(m-1)}}$ if it satisfies

$$x_{t+r_0\tau} \le x_{t+r_1\tau} \le \cdots \le x_{t+r_{m-1}\tau}, \quad (8)$$

where $0 \le r_i \le m-1$ and $r_i \ne r_j$

(iii) There are $m!$ possible permutations of an m-tuple vector. For each permutation π, the relative frequency is determined by

$$p(\pi) = \frac{\text{number}\left\{t \middle|_{t \le T-(m-1)\tau}, x_t^m \text{ has type } \pi\right\}}{N-(m-1)\tau}. \quad (9)$$

(iv) The PE of m dimension is then defined as

$$H_{\text{PE}}(m) = -\sum p(\pi) \ln(p(\pi)). \quad (10)$$

(v) The maximum value of $H_{\text{PE}}(m)$ is $\log(m!)$ when all possible permutations appear with the same probability. Therefore, the normalized permutation entropy (NPE) can be expressed as

$$H_{\text{NPE}}(m) = H_{\text{PE}} \frac{m}{1} \ln(m!). \quad (11)$$

For any time series, $0 \le H_{\text{NPE}}(m) \le 1$ is satisfied. It can represent randomicity and dynamic changes of the time series effectively: the smaller the value of $H_{\text{NPE}}(m)$ is, the more regular the time series is, and the larger the value of $H_{\text{NPE}}(m)$ is, the more random the time series is. According to [9], a random white noise will have a PE close to 1, while a sinusoidal signal and an AM-FM signal will have a PE close to 0.

3. Method and Application

3.1. Introducing the Bilateral Permutation Entropy (BPE) for Measurement. The PE is introduced into the PEEMD method to measure the chaos degree in a single IMF to eliminate mode mixing. However, another problem is that a real signal may be segmented into multiple IMF components that must be measured and eliminated [22]; there is a given assumption for illuminating the principle of mode splitting. Suppose a simulation signal (a white nose signal or some other signal) is decomposed into two or more IMF components under the condition that the PE value of every IMF should be lower than the given threshold. Two conclusions would be drawn. First, the PE value of the IMF that includes mode splitting would be larger than the IMF that includes just the single real signal because the chaos of IMF is increased by mixing the real signal with the segmentation of other signals. Second, if the PE value of the synthetic signal that has been decomposed into two or more IMFs is lower than some ingredient IMF, then some real signal would be split into multiple IMFs. The two conclusions would be effective on the condition that the multiple IMFs into which the real ingredient signal decomposed are weakly correlated with each other. The paper proposes the bilateral permutation entropy (BPE) index for estimating the degree of mode splitting in the IMFs of the targeted signal based on this condition.

As a hypothesis, the targeted time series signal is composed of low correlative signals. The BPE index is defined as follows:

$$\text{BPE}_{ij} \frac{\text{PE}_{ij}}{\text{PE}_i}, \quad (12)$$

where PE_i denotes the PE value of the ith IMF component after decomposition via the PEEMD and PE_{ij} indicates the PE value of the synthetic signal comprising the ith and jth IMF components. There are two domains of BPE_{ij} values.

In essence, the synthetic signal is reconstructed by the ith and jth IMF components. $\text{BPE}_{ij} \ge 1$ represents that the chaos degree of the synthetic signal is higher than that of the signal IMF; that is, there is no signal compatibility between the ith and jth IMF components. In terms of the decomposition of the targeted signal, the mode of a target signal is not split into the IMF components. By contrast, $\text{BPE}_{ij} < 1$ signifies that the chaos degree of the synthetic signal is lower than that of the signal IMF component. This can be largely attributed to the fact that the chaos signal has been offset against the compatibility between the IMFs; hence, there is mode splitting in the decomposition.

3.2. The Reconstruction and Elimination. First, the paper analyzes the mechanism of mode splitting and selects the measurement index for eliminating it. Then, it reconstructs the IMFs, the BPE values of which are less than 1. Nevertheless, the IMFs with a BPE value that is larger than 1 remain or the IMFs with the maximum BPE values are retained. Next, the reconstruction signal is decomposed via the PEEMD method, and the BPE values of the second-level IMFs are calculated until all of them exceed 1 within the number of the original ingredient components. The remaining IMFs are the decomposition results restraining mode splitting by the PEEMD. The process of eliminating mode splitting is as follows (Figure 1).

3.3. Simulation Signal Analysis

3.3.1. Simulation Signal Set. To describe the process of the measurement and elimination of mode splitting, typical synthetic signals are utilized in the comparative analysis. The signal S_1 consists of a Gaussian white noise signal, a high-frequency sinusoidal signal, a low-frequency sinusoidal signal, and an amplitude modulation signal (Figure 2). This paper assumes that the number of the sampling data is

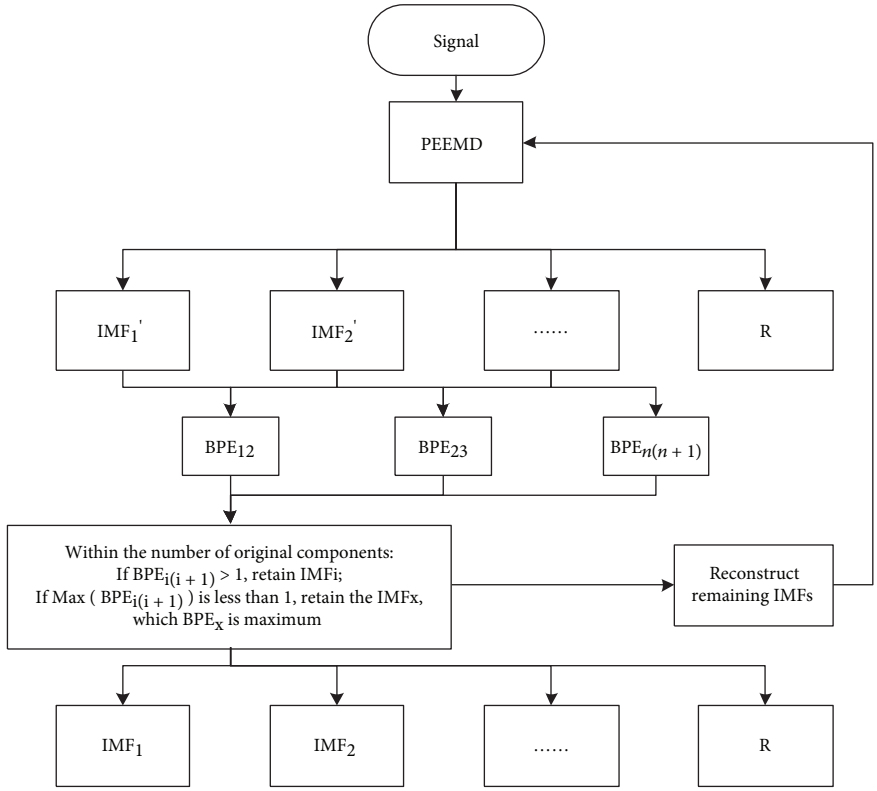

Figure 1: The scheme for eliminating mode splitting based on the PEEMD and BPE.

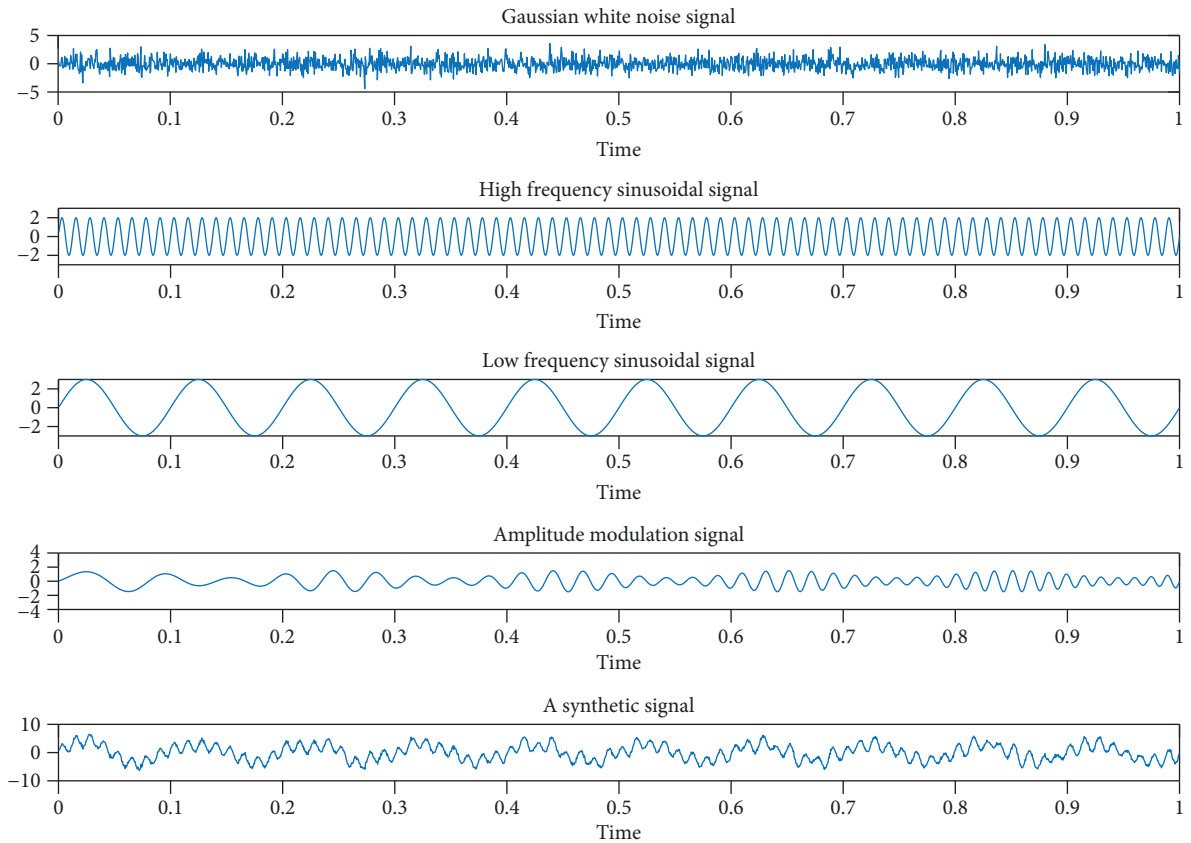

Figure 2: A synthetic signal S_1.

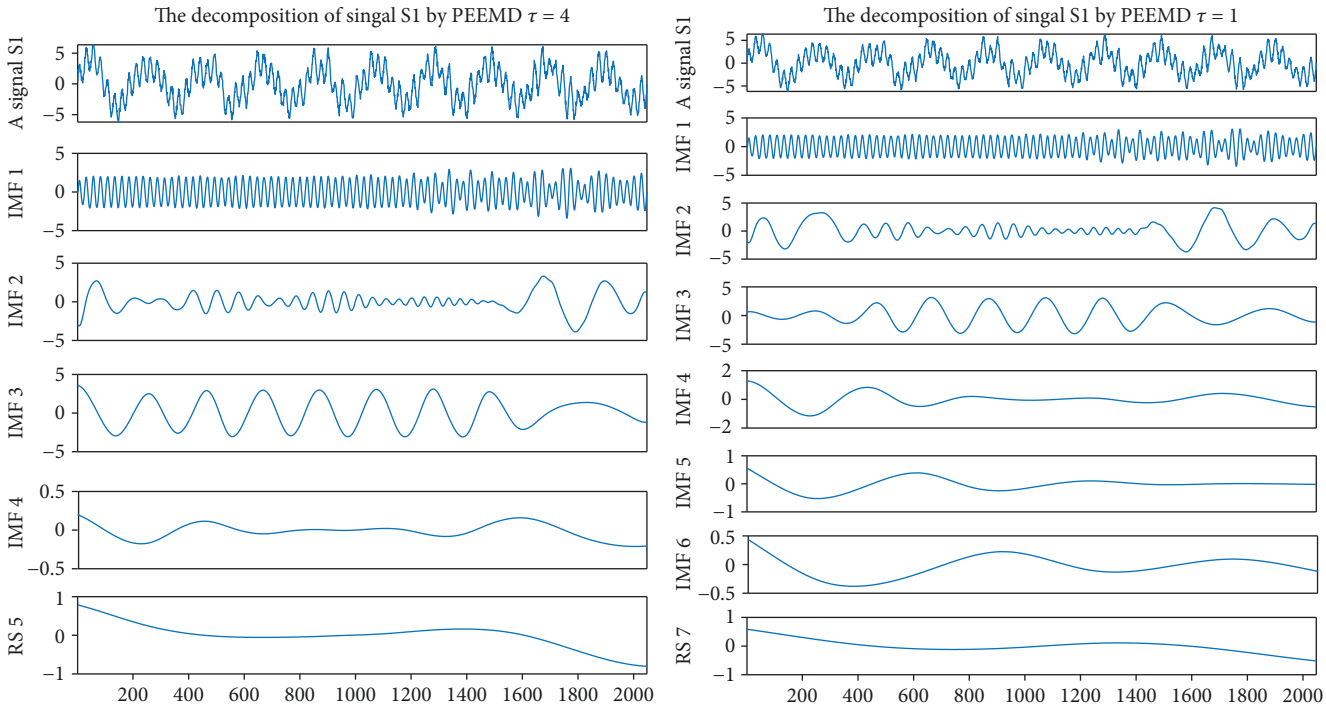

Figure 3: The decomposition of signal S_1 via the PEEMD method with $\tau = 4, 1$.

Table 1: Parameters in the PEEMD.

Cont.	NStd	MaxIter	Ne	τ	Mode	Thr
Value	0.2	6	50	4, 1	6	0.6

Footnotes: the symbols "NStd," "MaxIter," "Ne," "τ," "Mode," and "Thr" denote the noise standard deviation, maximum number of sifting iterations allowed, pair number of added white noise, delay time of permutation entropy, order of permutation entropy, and threshold of PE_j, respectively.

2048. The ingredient signals have a low correlation with each other.

$$\begin{aligned} GW &= wgn(1, N, 0.2), \\ LF &= 3^* \sin(2^*\pi^*80^*t), \\ HF &= 2^* \sin(2^*\pi^*80^*t), \\ AM &= 1 + (1 + 0.5^* \sin(2^*\pi^*5^*t)) \\ &\quad * \sin(2^*\pi^*30^*t\text{^}2 + 2^*\pi^*10^*t), \\ S_1 &= 0.3^*GW + HF + HF + AM, \end{aligned} \tag{13}$$

where $N = 2048$ and $t = 1/N : 1/N : 1$. Moreover, $t = 1/N : 1/N : 1$ denotes that the t value ranges between $1/N$ and 1, with an increase of $1/N$ in each step.

3.3.2. PEEMD and BPE Application. The IMFs of the S_1 based on the PEEMD are illustrated in Figure 3; the relevant parameters are shown in Table 1. Figure 3 shows that the IMF_1, IMF_2, and IMF_3 of the signal S_1 are partly similar to the original signals composing the synthetic signal S_1. Moreover, it is clear that the parts of the three IMFs are intertwined. Hence, the problem of mode splitting arises, and the paper quantitatively calculates the BPE value to tackle this issue.

To estimate the effectiveness of the BPE method under the same condition, the paper uses the same parameters in the BPE process. The results are shown in Figure 4. The minimum value among IMF_1, IMF_2, and IMF_3 is 0.93 or 0.8828, while the τ value is 1 or 4; this shows that there is some mode splitting under the current state of decomposition.

3.3.3. Results. According to the results (Figures 5 and 6), when the τ value is 4, the PE value of the reconstructed S_1 signal is slightly lower than the PE value of the original IMFs; this means that the randomicity and dynamic changes of the initial IMFs are treated to a certain degree of inhibition after reconstruction, and all the BPE values are obviously larger than 1; this denotes that the mode splitting problem is retained with the state of decomposition via PEEMD. The IMFs after reconstruction are not completely the same as the ingredient components, with the conditions that the BPE value is improved significantly and the PE value is retained partly. The reasons for this is that the IMF_1 that remained is not the same as the high-frequency sinusoidal signal; some residue signals, because of the mode splitting problem via PEEMD, are retained in the last part, and the IMF_1 will certainly lead to the next IMFs.

When the τ value is 1, the accumulation of mutual interference is obvious according to the results (Figures 5 and 6). The BPE_{12} and BPE_{34} values are near to the original BPE value, but the BPE_{23} value is just 0.477, which is sharply lower than the original BPE value (0.93). In addition, the PE value of the reconstructed IMF_2 (0.3791) is larger than the initial PE value of IMF_2. The PE value of the reconstructed

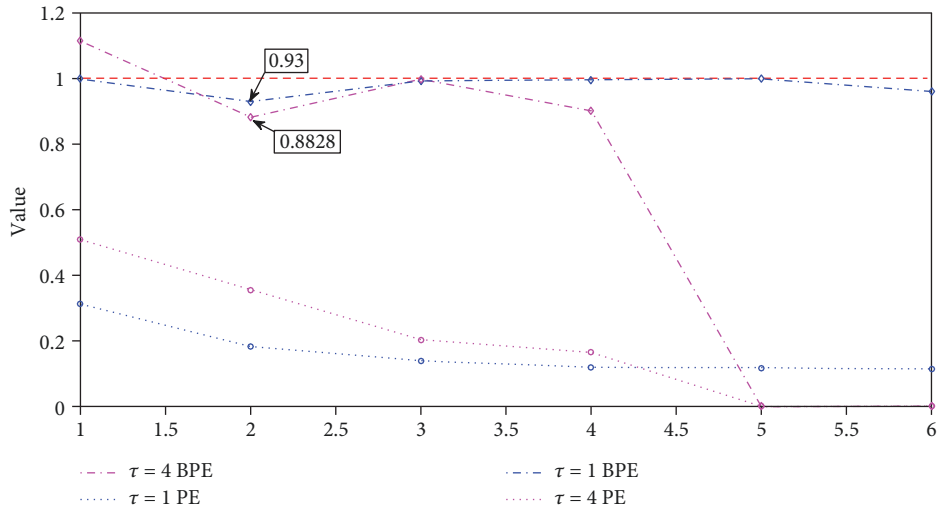

Figure 4: BPE and PE value of the IMFs in decomposition of S_1 signal $\tau = 4, 1$.

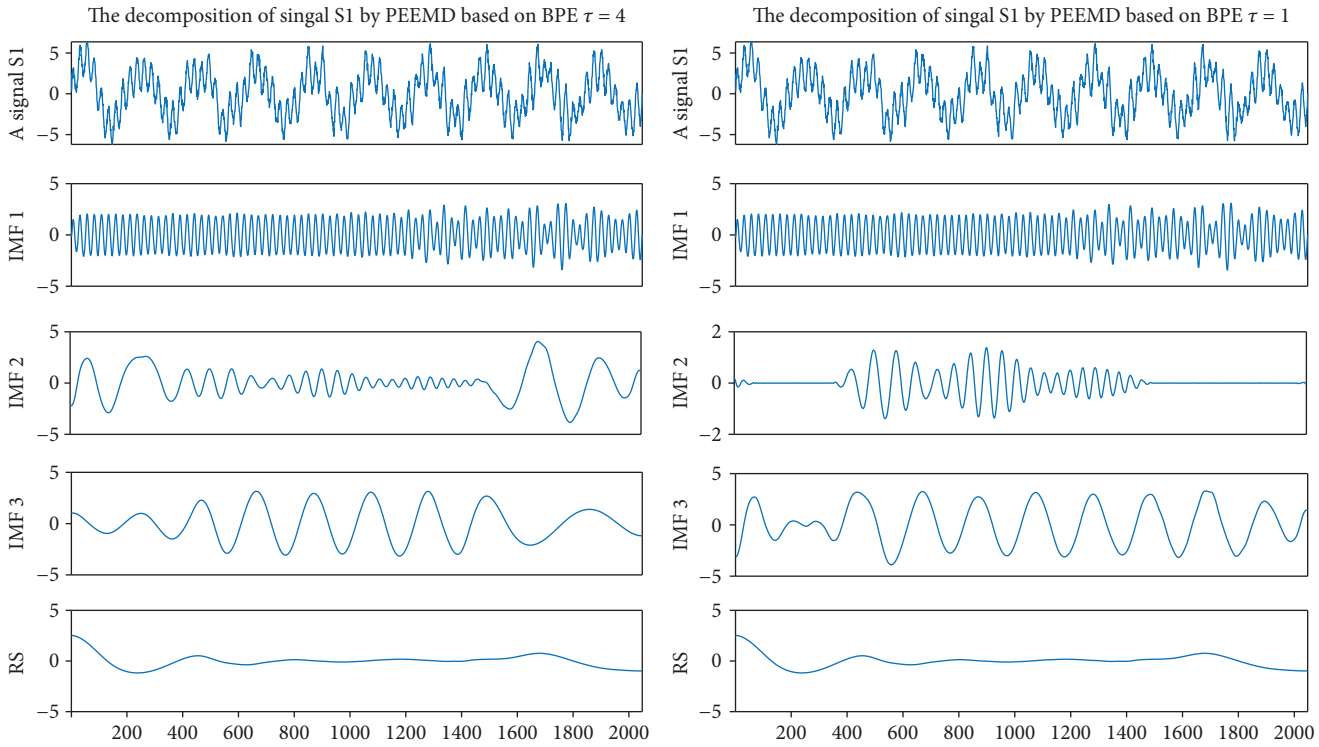

Figure 5: The decomposition of reconstructed signal S_1 via the PEEMD method $\tau = 4, 1$.

IMF_2 denotes that IMF_2 after reconstruction also has a serious mode-splitting problem with IMF_3 and that the randomicity and dynamic changes of IMF_2 are more serious. The same results are obtained intuitively from comparing Figure 3 with Figure 4.

The decomposition and reconstruction of the synthetic signals via PEEMD show that BPE can effectively reveal the degree of mode splitting in IMFs in a numerical, quantitative way. The elimination of mode splitting can be gradually improved and relies on the decomposition method and the choice of initial IMF.

3.4. Real Microseismic Data Processing. To test the BPE index effectiveness and feasibility in measured data, the microseismic signals are decomposed and reconstructed by PEEMD with BPE index. Figure 7 shows the decomposition of the microseismic signals from the shale gas project in Yibin City, Sichuan Province, China. The sampling step of this microseismic event is 0.004 s, and there are 8000 sampling points.

According to Figure 7, the microseismic signals contain mainly the first five IMFs, which are relative high-frequency IMFs. Therefore, the next decomposition of the reconstructed microseismic signals based on BPE value will

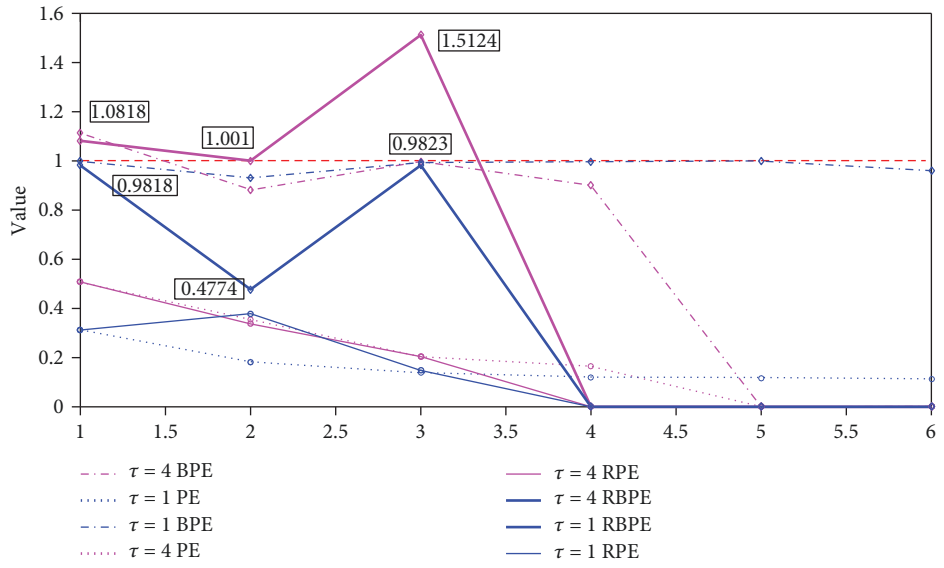

Figure 6: BPE and PE value of the IMFs in decomposition of reconstructed S_1 signal $\tau = 4, 1$.

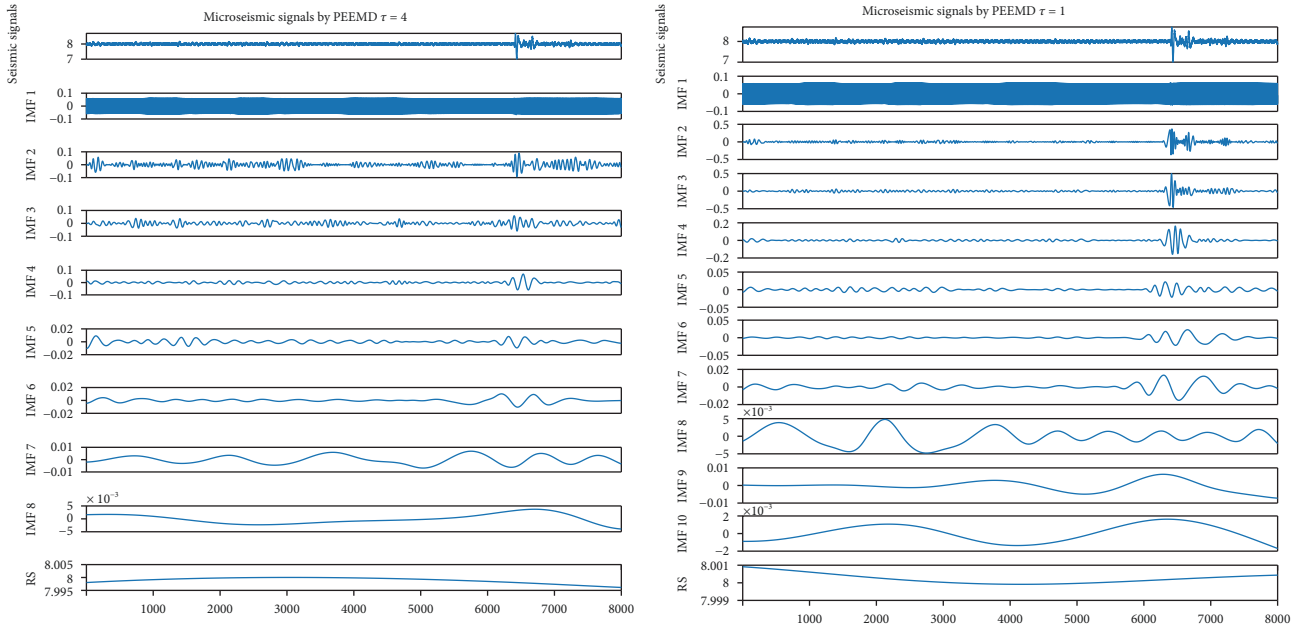

Figure 7: The decomposition of microseismic signals via the PEEMD method with $\tau = 4, 1$.

analyze the first five IMFs comparatively. The results of decomposition of the reconstructed microseismic signals based on the BPE value are shown in Figure 8.

According to the perspective of the time-domain diagram of the reconstructed microseismic signals (Figure 8) compared with the initial decomposition (Figure 7), the time is closed to each IMF when the amplitude is highest; this finding indicates that some incident occurred at that time. To briefly display the effect of gradually eliminating the influence of the mode-splitting phenomenon in the real measured data, the Fourier transform is required to address the time-domain diagram (Figure 9) when the delay time of permutation entropy is 4. The frequency distribution of amplitude peak in frequency-domain diagrams is extracted in Table 2. The frequency value of IMF_2 and IMF_3 in reconstructed signals is 3.5706 and 3.8452, respectively, which is from reconstructed components discarding IMF_3 and IMF_4. From the perspective of the frequency distribution characteristics, the frequency of reconstructed components dispersed more intensely to the center frequency. This finding suggests that the incident frequency is carried out in a more detailed decomposition in the frequency domain after the signal is reconstructed. That is, under the premise of the same decomposition methods (PEEMD), signal interference of the frequency domain is smaller in IMFs. The mode-splitting phenomenon is restrained to some extent.

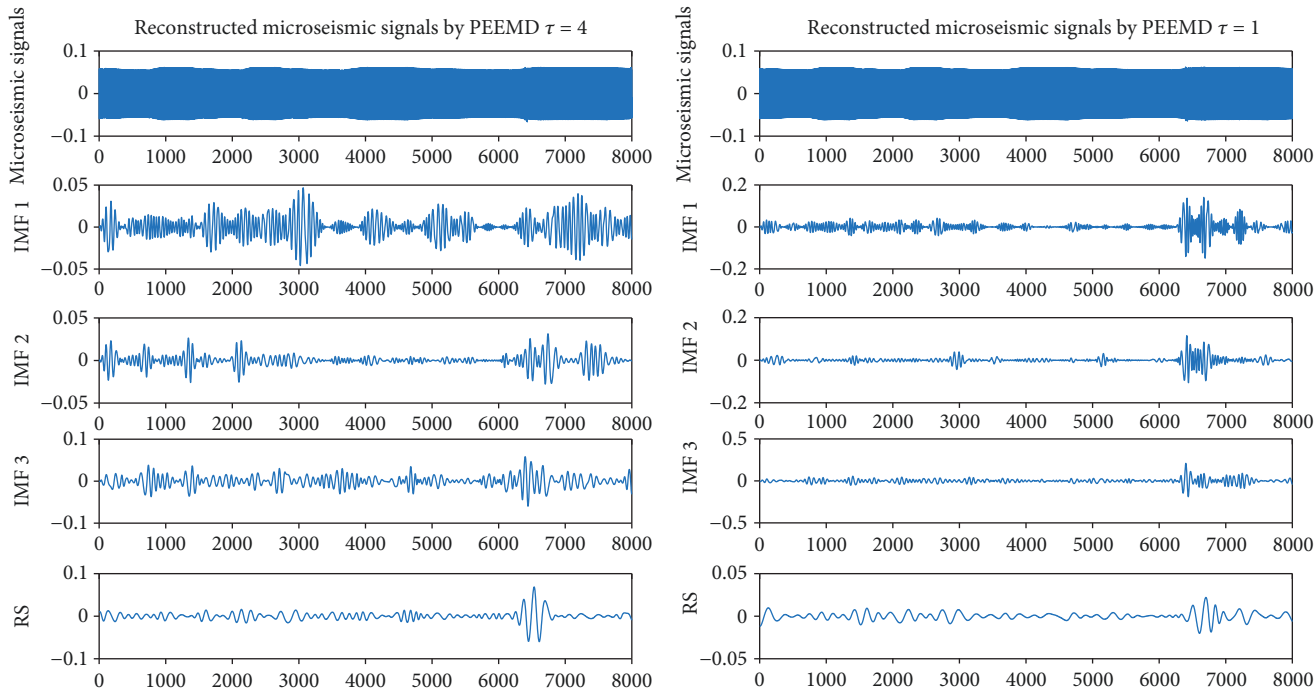

Figure 8: The decomposition of reconstructed microseismic signals via the PEEMD method with $\tau = 4, 1$.

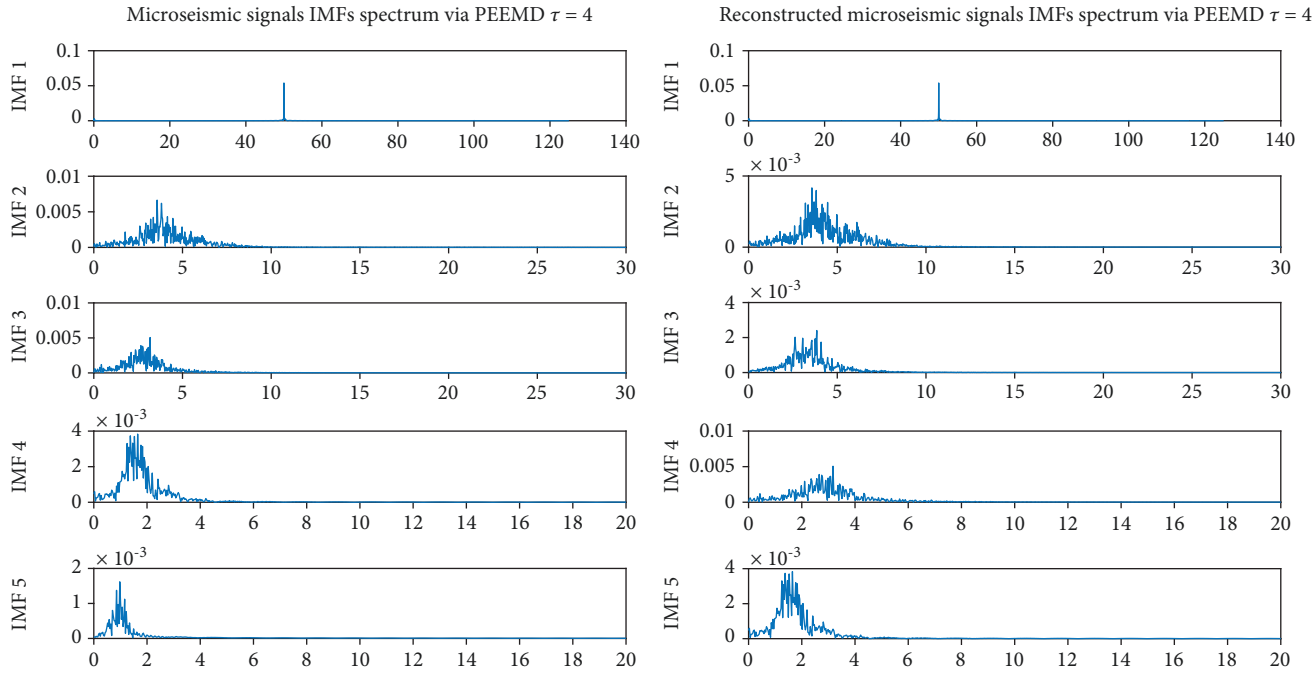

Figure 9: The spectrum of microseismic signals and reconstructed signals based on BPE index with $\tau = 4$.

4. Conclusion

After reviewing the principle of the PEEMD algorithm and the PE algorithm in this paper, a new method for measuring mode splitting and a new process of eliminating mode splitting are proposed, first based on the decomposition results obtained via the PEEMD method. Despite utilizing the synthetic signals, the minimum BPE_{23} value is 0.4774, which is not close to the standard value; the minimum BPE_{23} value is even is lower than the initial IMFs decomposed by the PEEMD when the delay time of permutation entropy is 1. Based on the intuitive comparative of the minimum BPE_{23} value with the IMFs, the PEEMD method (via the BPE index) shows that the degree of the mode-splitting problem is consistent with the IMFs, regardless of the degree of mode splitting that the PEEMD (after reconstructing signals based

Table 2: The frequency value on the maximum amplitude in each IMF.

Cont.	IMF_2	IMF_3	IMF_4	IMF_5	Mean	Std.
Value O	3.5706	3.1738	1.6479	0.9766	2.3422	1.0663
Value R	3.5706	3.8452	3.1738	1.6479	2.4475	1.0466

Footnotes: the symbols "Value O," "Value R," "Mean," and "Std." denote the frequency value in the initial microseismic signals, the frequency value in the reconstructed microseismic signals, the mean value of the frequency value, and the standard deviation, respectively.

on the BPE index) can alleviate or aggravate. This method shows that the BPE index is an effective measurement tool to detect mode splitting.

The microseismic signal is applied in this method to measure and eliminate the mode-splitting problem. The results are more specially analyzed by the Fourier-transform. When the delay time of the permutation entropy is 4, the statistical characteristics of the frequency value on the maximum amplitude denote the discrete degree of the incident frequency after reconstruction is lower. Thus, the IMFs of the reconstructed signals are closer to the real incident frequency value.

The components of the IMFs are not completely the same as the synthetic components in this paper, because the gradual elimination of the mode splitting is affected by the decomposition method parameters and the first IMF treated as the benchmark. Nonetheless, these components are significantly meaningful for the signal quantitative analysis regarding the elimination of mode splitting.

Appendix

Main code

```
%% calculate BPE value
imfpeemd=peemd(S,Nstd,Ne,MaxIter,Mode,τ,Thr);
% S:input signals; Nstd: noise standard deviation; Ne: number of realizations;
% MaxIter: maximum number of sifting iterations allowed; Mode: order of permutation entropy;
%τ: delay time of permuation entropy; Thr: threshold of permuation entropy
tempimf=imfpeemd;
[a,b]=size(imfpeemd);
% calculate PE and calculate BPE
for i=1:1:a-1
[c,d]=size(imfpeemd);
tempe=zeros(c-1,3);
for k=1:1:c-1
tempe(k,1)=pec(imfpeemd(k,:),Mode,τ) % function PE
tempe(k,2)=pec(imfpeemd(k,:)+imfpeemd(k+1,:),
Mode,τ);
tempe(k,3)=tempe(k,2)/tempe(k,1);
end
%%function PEEMD
function modes=peemd(S,Nstd,Ne,MaxIter,Mode,τ,Thr)
% standardization
desvio_x=std(x);
x=x/desvio_x;
modes=zeros(size(x));
aux=zeros(MaxIter+1,size(x,2));
acum=zeros(size(x));
% generate the noise signals
for i=1:Ne.
    white_noise{i}=randn(size(x));
end;
while nnz(diff(sign(diff(x-acum))))>2
% Generate the IMF and calculate the mean
    for i=1:Ne.
        [temp1, o1, it1]=emd(x-acum+Nstd*white_
        noise{i},'MAXITER',MaxIter);
        [temp2, o2, it2]=emd(x-acum-Nstd*white_-
        noise{i},'MAXITER',MaxIter);
        te=min(size(temp1,1),size(temp2,1));
        if te==MaxIter+1
            aux=aux+(temp1+temp2)./(2*Ne);
        else
            temp1(te+1:MaxIter+1,:)=0;
            temp2(te+1:MaxIter+1,:)=0;
            aux=aux+(temp1+temp2)./(2*Ne);
        end
end
% Calculate the PE of the IMFs
    for i = 1:size(temp1,1)
    auxPE=pec(aux(i,:),Mode,τ);
    if auxPE>=Thr
        acum=acum+aux(i,:);
    end
end
% decompose the Residual signal by EMD
        modes=emd(x-acum); % function emd
    break
end;
% restore the original level
modes=modes*desvio_x;
end
```

Data Availability

This paper selects the simulation signal for empirical analysis and does not contain specific data.

Conflicts of Interest

The authors declare no conflict of interest.

Acknowledgments

This paper was supported by the National Key R&D Program of China (2018YFC0604105), Opening Fund of Geomathematics Key Laboratory of Sichuan Province (Project no. scsxdz201601), and Scientific Research Fund of Education Department in Sichuan (Project nos. 17ZB0046 and 18ZB0062).

References

[1] Z. Wu and N. E. Huang, "A study of the characteristics of white noise using the empirical mode decomposition method," *Proceedings of the Royal Society A: Mathematical, Physical and Engineering Sciences*, vol. 460, no. 2046, pp. 1597–1611, 2004.

[2] H. Huang and J. Pan, "Speech pitch determination based on Hilbert-Huang transform," *Signal Processing*, vol. 86, no. 4, pp. 792–803, 2006.

[3] N. E. Huang, Z. Shen, S. R. Long et al., "The empirical mode decomposition and the Hilbert spectrum for nonlinear and non-stationary time series analysis," *Proceedings of the Royal Society A: Mathematical, Physical and Engineering Sciences*, vol. 454, no. 1971, pp. 903–995, 1998.

[4] P. Goncalves, P. Abry, G. Rilling, and P. Flandrin, "Fractal dimension estimation: empirical mode decomposition versus wavelets," in *2007 IEEE International Conference on Acoustics, Speech and Signal Processing - ICASSP '07*, vol. 3, pp. 1153–1156, Honolulu, HI, USA, April 2007.

[5] P. Flandrin, G. Rilling, and P. Goncalves, "Empirical mode decomposition as a filter bank," *IEEE Signal Processing Letters*, vol. 11, no. 2, pp. 112–114, 2004.

[6] X. Li, "Temporal structure of neuronal population oscillations with empirical model decomposition," *Physics Letters A*, vol. 356, no. 3, pp. 237–241, 2006.

[7] Z. Wu and N. E. Huang, "Ensemble empirical mode decomposition: a noise-assisted data analysis method," *Advances in Adaptive Data Analysis*, vol. 1, no. 1, pp. 1–41, 2009.

[8] J.-R. Yeh, J.-S. Shieh, and N. E. Huang, "Complementary ensemble empirical mode decomposition: a novel noise enhanced data analysis method," *Advances in Adaptive Data Analysis*, vol. 2, no. 2, pp. 135–156, 2010.

[9] J. Zheng, J. Cheng, and Y. Yang, "Partly ensemble empirical mode decomposition: an improved noise-assisted method for eliminating mode mixing," *Signal Processing*, vol. 96, pp. 362–374, 2014.

[10] C. Bandt and B. Pompe, "Permutation entropy: a natural complexity measure for time series," *Physical Review Letters*, vol. 88, no. 17, article 174102, 2002.

[11] S. M. Pincus, "Approximate entropy as a measure of system complexity," *Proceedings of the National Academy of Sciences of the United States of America*, vol. 88, no. 6, pp. 2297–2301, 1991.

[12] J. S. Richman and J. R. Moorman, "Physiological time-series analysis using approximate entropy and sample entropy," *American Journal of Physiology-Heart and Circulatory Physiology*, vol. 278, no. 6, pp. H2039–H2049, 2000.

[13] R. Gu, "Multiscale Shannon entropy and its application in the stock market," *Physica A: Statistical Mechanics and its Applications*, vol. 484, pp. 215–224, 2017.

[14] L. Z. Liu, X. Y. Qian, and H. Y. Lu, "Cross-sample entropy of foreign exchange time series," *Physica A: Statistical Mechanics and its Applications*, vol. 389, no. 21, pp. 4785–4792, 2010.

[15] A. A. Bruzzo, B. Gesierich, M. Santi, C. A. Tassinari, N. Birbaumer, and G. Rubboli, "Permutation entropy to detect vigilance changes and preictal states from scalp EEG in epileptic patients. A preliminary study," *Neurological Sciences*, vol. 29, no. 1, pp. 3–9, 2008.

[16] R. Sinatra and M. Szell, "Entropy and the predictability of online life," *Entropy*, vol. 16, no. 1, pp. 543–556, 2014.

[17] L. Zunino, M. Zanin, B. M. Tabak, D. G. Pérez, and O. A. Rosso, "Forbidden patterns, permutation entropy and stock market inefficiency," *Physica A: Statistical Mechanics and its Applications*, vol. 388, no. 14, pp. 2854–2864, 2009.

[18] K. Xu and J. Wang, "Weighted fractional permutation entropy and fractional sample entropy for nonlinear Potts financial dynamics," *Physics Letters A*, vol. 381, no. 8, pp. 767–779, 2017.

[19] S. D. Wu, P. H. Wu, C. W. Wu, J. J. Ding, and C. C. Wang, "Bearing fault diagnosis based on multiscale permutation entropy and support vector machine," *Entropy*, vol. 14, no. 8, pp. 1343–1356, 2012.

[20] R. Li and J. Wang, "Interacting price model and fluctuation behavior analysis from Lempel–Ziv complexity and multi-scale weighted-permutation entropy," *Physics Letters A*, vol. 380, no. 1-2, pp. 117–129, 2016.

[21] L. Hussain, W. Aziz, S. Saeed et al., "Complexity analysis of EEG motor movement with eye open and close subjects using multiscale permutation entropy (MPE) technique," *Biomedical Research*, vol. 28, pp. 7104–7111, 2017.

[22] G. Wang, X.-Y. Chen, F.-L. Qiao, Z. Wu, and N. E. Huang, "On intrinsic mode function," *Advances in Adaptive Data Analysis*, vol. 2, no. 3, pp. 277–293, 2010.